ANNALS OF GEOPHYSICS, 65, 5, DM532, 2022; doi:10.4401/ag-8736
OPEN ACCESS

Refining micro-seismic catalogs around Seydişehir, Turkey

Evrim Yavuz*,[1]

(1) Istanbul Metropolitan Municipality, Department of Earthquake Risk Management and Urban Improvement, Directorate of Earthquake and Geotechnical Investigation, 34134, Bakırköy, Istanbul, Turkey

Article history: received September 21, 2021; accepted May 16, 2022

Abstract

In Turkey, two official seismology centers, Bogazici University Kandilli Observatory and Earthquake Research Institute Regional Earthquake-Tsunami Monitoring Center (KOERI-RETMC) and Republic of Turkey Prime Ministry Disaster Emergency Management Authority (AFAD) announce and share seismic catalogs with the public and international services. According to their seismic network distribution, together with different crustal models and calculation algorithms, obtaining earthquake parameters (location, depth, etc.) could differ between these two centers, especially, affecting source types of the low-magnitude events. Both low-magnitude tectonic events and artificial quakes that originating from open-pit quarry are catalogued by the seismology centers. These two centers announce different source types for the seismic events; therefore, this study focuses on the reliable identification of the micro-seismic events. Magnitude Ml<2.4 177 seismic events commonly identified in KOERI-RETMC and AFAD catalogs are used. Due to the differences between KOERI-RETMC and AFAD seismic catalogs, the "first determination" (FD) was needed to start the discrimination analyses. Then, waveforms of the station SEYD and SEDI are operated by KOERI-RETMC and AFAD were analyzed with four methods (Amplitude Ratio, Complexity, Short Time Fourier Transform and Corner Frequency-Power Spectrum) and two statistical approaches (linear and quadratic discriminant functions) with the use and comparison with FD. Finally, station-based weightings are obtained with all techniques, and the source types of all events are calculated in percent. Generally, the success rates of the methods are calculated over 90%. The reliability increases with the co-usage of many analyses and the application of method-based weighting. Hence, many methods should be used to reliably determine the source types of micro-seismic events. Both centers should make more detailed analyses to identify micro-seismic events and share their reliable and revised catalogs.

Keywords: Discrimination methods; Seismic catalogs; Source type identification; Statistical approaches; Turkey

1. Introduction

The study area, Seydişehir district, is positioned in the southwestern part of Turkey. There is no active fault within the study area; however, on the northeastern side, the N-S directional normal Alacadağ Fault Zone, which is

the closest tectonic feature to the region, is lying. Besides, this area is tectonically situated within the Isparta Angle and a lake region. Therefore, riedel fractures, local faults and folds are present around the region and might produce low-magnitude earthquakes [Emre et al., 2013; http://yerbilimleri.mta.gov.tr/anasayfa.aspx] (Figure 1). Jurassic-Cretaceous limestones are dominant in the study area, and the presence of Paleocene-Eocene clastic and carbonates, Mesozoic peridotites and Carboniferous flysch are encountered [Akbaş et al., 2011]. Also, collapse earthquakes could be recorded since karstification is observed in the region using the geological structure and groundwater. There is only one open-pit quarry in this region to obtain materials from limestones. Hence, the quarry blast activity has been for many years and could occur low-magnitude quakes. They may contaminate the earthquake catalogs if they cannot be identified by the seismology centers, leading to erroneous seismological studies.

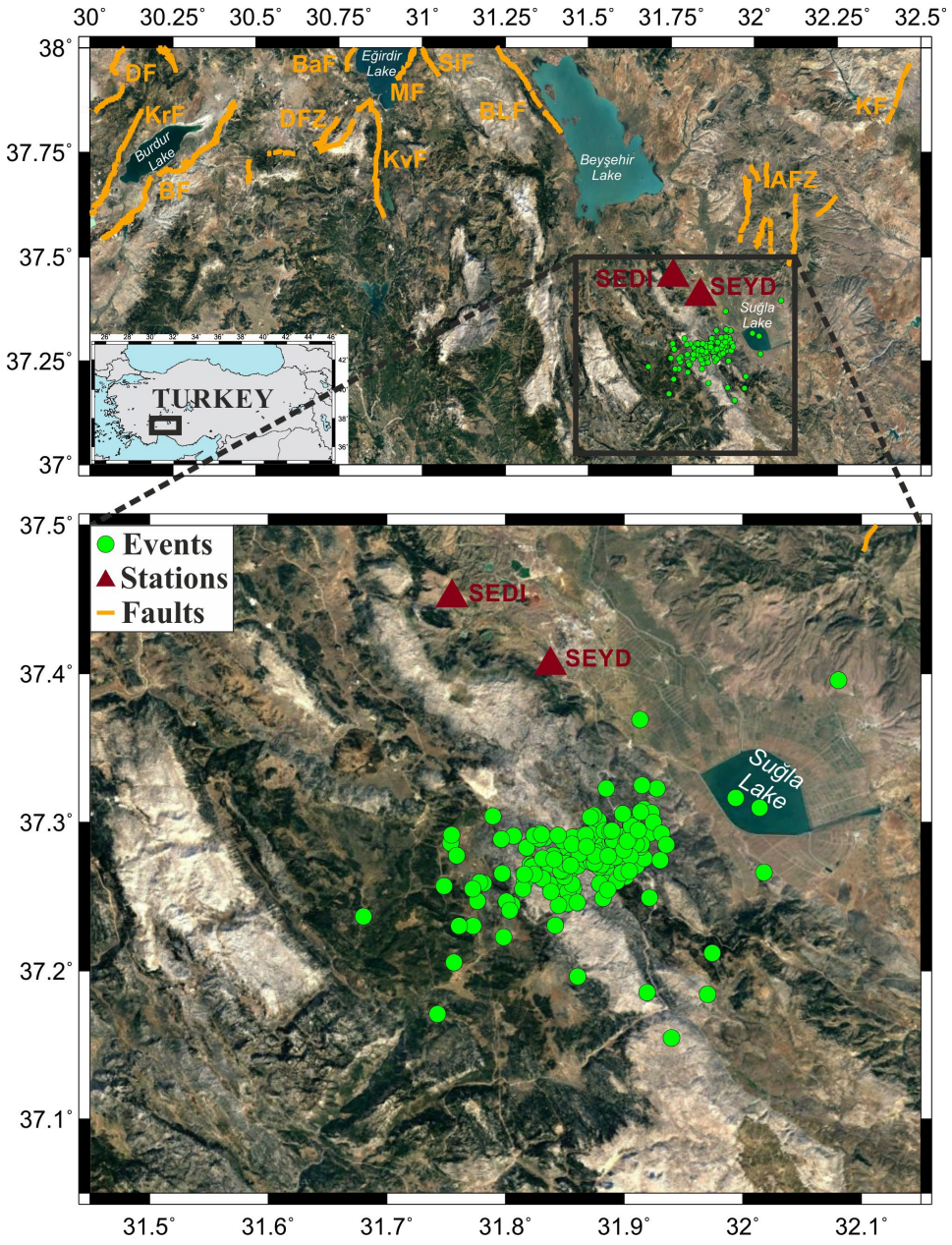

Figure 1. The map showing some part of structural elements of the Isparta Angle and Seydişehir region. The black quadrilaterals demonstrate the study area with broad and general perspectives. The locations of the seismic events (average coordinates of both KOERI-RETMC and AFAD) and the stations used in this study depict with the green circles and bordeaux triangles, respectively. The orange lines indicate the active faults (Emre et al., 2013). AFZ: Alacadağ Fault Zone, BF: Burdur Fault, BaF: Barla Fault, BLF: Beyşehir Lake Fault, DF: Dinar Fault, DFZ: Davras Fault Zone, KF: Konya Fault, KrF: Karakent Fault, KvF: Kovada Fault, MF: Mahmatlar Fault, SiF: Sarıidris Fault.

Various researchers have carried out the determination of the source types of artificial and natural quakes using many different methods. Hedlin et al. [1989] characterized the records of the blasts and earthquakes in the time and frequency domain in Kazakhstan. Baumgardt and Young [1990] analyzed the source types of the record by using *P*n/*S*n, *P*n/*Lg*, and their spectral ratios in Norway. Quarry blasts and mine explosions were distinguished from earthquakes using coda waves and power spectra in the United States [Su et al., 1991]. The *P* and *S* wave amplitude ratio method used by Wüster [1993] to discriminate the chemical explosions and natural quakes. Gitterman and Shapira [1993] used complexity and spectral ratio techniques to identify underwater explosions and earthquakes. In Israel, the source types were identified by using spectra with different epicentral-distanced quakes [Gitterman and Eck, 1993]. Kim et al. [1994] discriminated the chemical explosions and earthquakes by using high frequency spectra. Aki [1995] was performed the power spectral density and coda wave decay techniques in the United States. In South America, Beck and Wallace [1997] analyzed the source types of the seismic events by using the amplitude ratio and time-frequency domain methods together. Gitterman et al. [1998] used amplitude ratio method for the Middle East by using lots of crustal or underwater seismic events. The spectrograms of the high frequency quakes were analyzed by Carr and Garbin [1998] in the United States. The amplitude ratio and complexity methods were jointly used with some linear or non-linear statistical approaches in the identification of the source types of the micro-seismic events [Koch and Fäh, 2002; Arai and Yoshida, 2004; Horasan et al., 2009; Kartal and Horasan, 2011; Öğütçü et al., 2011; Kekovalı et al., 2012; Tibi et al., 2018a; Tibi et al., 2018b; Badawy et al., 2019; Pyle and Walter, 2019]. The categorization of the seismic events was determined by time-frequency methods as Wavelet Transform, Short Time Fourier Transform, corner frequencies, or power spectrum. Using different techniques could improve the success rate of the identification, especially for both time and frequency methods [Roueff et al., 2004; Arrowsmith et al., 2006; Allmann et al., 2008; Yılmaz et al., 2013; Ataeva et al., 2017; Budakoğlu and Horasan, 2018; Yavuz et al., 2019a; Yavuz et al., 2019b; Sertçelik et al., 2020].

In this study, the "first determination" (FD) that visually determines with the *P* wave first motion polarity, no or low *S* wave phase, high amplitude of *P* wave, *Rg* phase appearance, coda wave decay rate, was observationally defined for 177 seismic events that have been cataloged on both Bogazici University Kandilli Observatory and Earthquake Research Institute Regional Earthquake-Tsunami Monitoring Center (KOERI-RETMC) and Republic of Turkey Prime Ministry Disaster Emergency Management Authority (AFAD). The source types were analyzed by four different methods (amplitude ratio, complexity, Short Time Fourier Transform and corner frequency of the power spectrum) and two statistical approaches (Linear and Quadratic Discrimination Functions) according to the two seismic stations that are operated by both seismological centers. The weight of each method was determined according to its success rate with a comparison of FD, and the determination of the source types of the events was calculated with the help of the weight. A joint study was conducted to correct the confusion that arose due to the different identification of the events in both centers.

2. Data set

One of the main separating features of artificial and natural quakes is the seismograms of vertical motion of seismic waves, especially the dominant *P* wave phase [Baumgard and Young, 1990; Gitterman et al., 1998; Horasan et al., 2009; Korrat et al., 2022]. Therefore, the vertical components of the station SEYD and SEDI, which are operated by KOERI-RETMC and AFAD, respectively were used for source type identification (Table 1). Both stations have a broadband sensor, and the sampling rates are set to 100 samples per second. The distance between these stations is about 8.91 km. The opening dates are Feb 3, 2014 for station SEYD, and Dec 1, 2014 for station SEDI.

Station Name	Latitude (oN)	Longitude (oE)	Elevation (m)	Opening Date	Sensor Type	Operator
SEYD	37.4056	31.8379	1160	03.02.2014	GURALP-40T	KOERI-RETMC
SEDI	37.4511	31.7549	1255	01.12.2014	GURALP-3T	AFAD

Table 1. The information of the seismic stations.

177 seismic events recorded both stations and cataloged on both centers are used for source type identification. Minimum and maximum distances are varied from 5.80 to 29.61 km for stations SEYD, and 7.39 to 32.96 km for station SEDI due to their operation center's catalog. Since the largest artificial quake in the region is Ml=2.4; hence, this magnitude is taken as a maximum for all events. 44 natural and 133 artificial events are identified by KOERI, where 149 natural and 28 artificial events are cataloged by AFAD (Appendix A). The difference of the event parameters is based on the crustal models, location algorithms, etc.; but the source types are determined by the operator. Due to this difference, the event types are separately evaluated manually using *P* wave first motion polarity, no or low *S* wave phase, high amplitude of *P* wave, *Rg* phase appearance, coda wave decay rate and it is called as "first determination" FD. For clear identification, the earthquake parameters (time, location, depth, and magnitude) are gained from both KOERI-RETMC and AFAD catalogs and taken as an average version to make a common point for FD. 9 natural and 168 artificial quakes are determined by FD (Appendix A). The event distribution is shown in Figure 2.

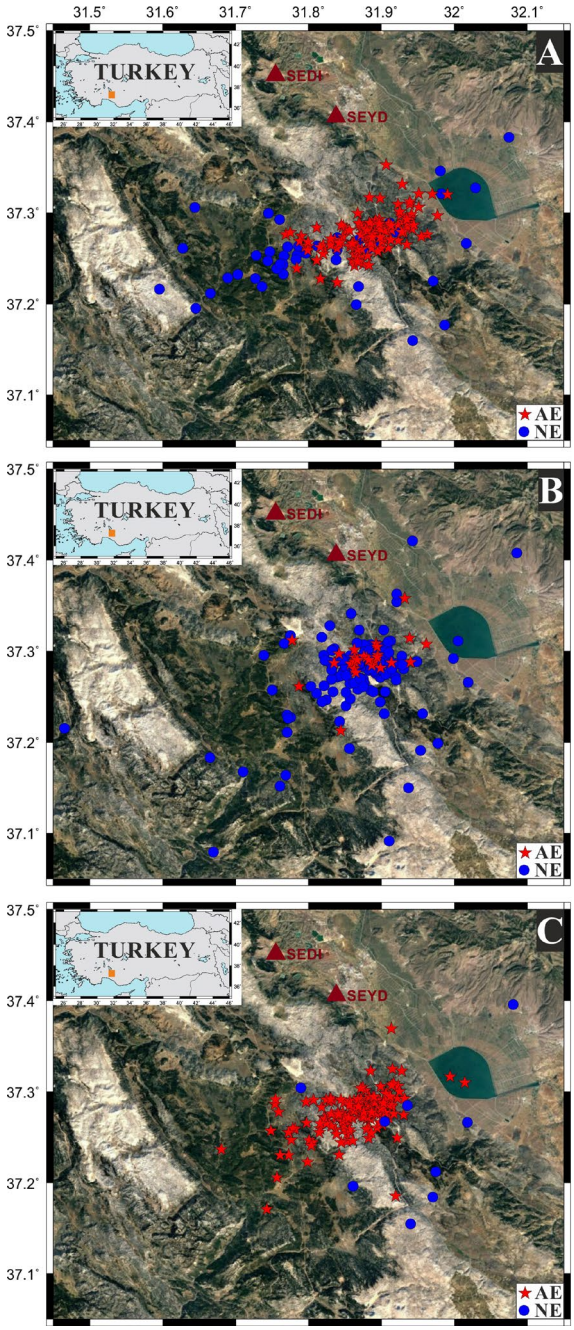

Figure 2. Event and source type distribution by A) KOERI-RETMC, B) AFAD and C) FD. AE: artificial events, NE: natural events.

The time and magnitude distribution according to KOERI-RETMC, AFAD and FD are shown in Figure 3.

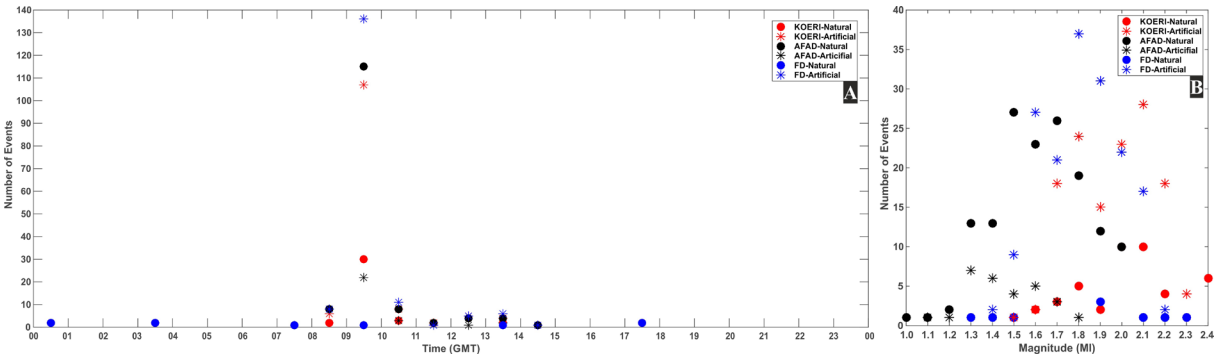

Figure 3. A) Time and B) Magnitude distributions of the natural and artificial events by KOERI-RETMC, AFAD and FD.

3. Methodology

Four different methods and two statistical approaches used in two of these methods were used for both seismic recordings of 177 seismic events. Firstly, all events are evaluated manually using some criteria based on both seismic station recordings, as it was mentioned in the previous section, "Data Set". This is the beginning of the event type identification to compare the methods and calculate the success rates.

The amplitude ratio method has been widely used for discriminating tectonic and artificial quakes. This method is based on the comparison the dominant amplitudes of *P* and *S* waves and the logarithm of the peak amplitude values of *S* waves [Wüster 1993; Baumgart and Young, 1990]. The easy and fast amplitude ratio analysis is used for source type determination since the amplitude of the S wave is higher than the *P* wave in tectonic events, and vice versa for artificial [Hedlin et al., 1990; Sertçelik and Başer, 2010; Öğütçü et al., 2011; Yavuz et al., 2019a; Tan et al., 2021].

The other technique is called complexity and it is based on the comparison between the ratio of powers of time windows (Complexity-C) and integrated spectral amplitudes (Spectral Ratio-Sr) (Eq. 1-2) [Kelly, 1968; Gitterman and Shapira, 1993]. The dominant frequencies of local tectonic events are variable, while it is much more constant for artificial quakes [Yılmaz et al., 2013; Budakoğlu and Horasan, 2018; Yavuz et al., 2019b].

$$C = \int_{t_1}^{t_2} s^2(t)dt / \int_{t_0}^{t_1} s^2(t)dt \tag{1}$$

$$Sr = \int_{h_1}^{h_2} a(f)df / \int_{l_1}^{l_2} a(f)df \tag{2}$$

In Eq. 1-2, t_0 and t_1 are *P* and *S* wave onset times, respectively. t_2 is calculated with the time interval of t_1-t_0, and addition of t_1. $s^2(t)$ is the spectral ratio of integrated powers, and $a(f)$ is the ratio of integrated spectral amplitudes. h_1, h_1, l_1 and l_1 are the corner frequencies and they were determined as 5, 10, 1, 5 Hz, respectively. While the epicentral distance changes, the signal characteristic is also altered due to the attenuation, scattering, etc. Especially, the signals of artificial quakes appear to be more complex at farther recordings due to this effect [Bormann, 2009; Stein and Wysession, 2009]. However, since calculations were made from the windows of the *P* and *S* wave phases in the complexity method, the effect of the dependence within the local distance limits could be eliminated. Thus, the dominant *P* and *S* amplitudes used in the amplitude ratio method and the values calculated from the windows dependent on the *P* and *S* wave phases in the complexity method show that the methods are in a strong relationship with each other, and reliable results could be obtained in the discrimination analyses.

Statistical approaches are needed to classify data in different groups created with different Gaussian distributions. As a result of a minimum classification error, Linear Discriminant Function (LDF) and Quadratic Discriminant

Function (QDF) are used, which define the new data classes of the first input data set defined as FD in this study [Fisher, 1936; Seber, 1984; Krzanowski, 1988; Franc and Hlavac, 2004; Tüysüz ve Yaylalı, 2005; Kuyuk et al. 2014]. One covariance matrix is estimated for all classes while using LDF, while for each class for QDF [Kuyuk et al., 2014].

According to the FD and calculated values through the amplitude ratio and complexity methods, the discrimination study uses Eq. 3-4.

$$F_{LDF} = K + [L] * \begin{bmatrix} x \\ y \end{bmatrix} \tag{3}$$

$$F_{QDF} = K + [L] * \begin{bmatrix} x \\ y \end{bmatrix} + [x \quad y] * [Q] * \begin{bmatrix} x \\ y \end{bmatrix} \tag{4}$$

where K is a constant, L and Q are linear and quadratic coefficient matrixes, respectively.

The other method is called Short Time Fourier Transform (STFT) and it is based on the visualization of the signal's amplitude on both time and frequency domains. The measure of the energy distribution over time and signal's frequency is defined as a spectrogram for STFT [Hedlin et al., 1989; Başokur, 2007]. The method shows the conjugation of time and frequency as a two-dimensional function by applying the Fourier Transform based on windowing on the signal [Beck and Wallace, 1997; Yılmaz et al., 2013]. Thus, the time-frequency-amplitude distribution can be displayed in detail with the specified window functions [Gabor 1946; Cohen 1989; Auger et al., 1996] (Eq. 5).

$$STFT(\tau, f) = \int f(t) g(t - \tau) e^{-i\omega t} dt \tag{5}$$

where $f(t)$ is a signal in the time domain; $g(t)$ is a window function.

The last method is the Corner Frequency of the Power Spectrum (CF-PS). The concept that expresses the intensity of the change of strong or weak energy along with the total energy on a given signal is called the Power Spectrum. The main purpose is based on the principle of squaring the values of the amplitudes of the window determined on a signal in the frequency domain [Bormann, 2009; Semmlow, 2012]. The corner frequency (f_c) is a boundary of a frequency response at energy begins to be reduced; in other words, the intersection of low and high frequencies [Brune, 1970; Bormann, 2009]. Focusing on the frequency content of events with different source types, discrimination analyzes can be performed with corner frequencies calculated over the power spectrum [Ataeva et al., 2017; Gaber et al., 2017]. The energy density of artificial events decreases more sharply towards increasing frequencies, while it is more stable on tectonic events [Su et al., 1991; Yavuz et al., 2019a]. All processes were done by MATLAB based codes. [Auger et al., 1996; Kuyuk et al., 2014; Yavuz et al., 2019a; Yavuz, 2021].

4. Results

This study evaluated the source types of 177 seismic events defined in AFAD and KRDAE-RETMC catalogs according to the FD to set out a common framework. Four methods and two statistical approaches used in two of these methods were jointly performed at station SEYD and SEDI.

In the beginning, the amplitude ratio and complexity methods were applied with the usage of LDF and QDF for both stations (Figure 4). When the analyzes were made according to the KOERI-RETMC or AFAD catalogs, it was observed that the discrimination functions could not classify the data. This reveals that the identified source types on the two catalogs are partially incorrect. On the other hand, the results of the amplitude ratio method could not provide the boundary conditions due to the first-order function of the LDF, and it cannot limit the scattered data. Thus, the classification process could not be achieved. When the discrimination functions are tried to be calculated based on the source type information in the KOERI-RETMC and AFAD catalogs, the equations could not limit the data and erroneous graphics were obtained. According to the results compared with the FD, LDF and QDF generally classify with a success rate of at least 91.53% (Table 2, Appendix A). Regardless of the number of data, both discrimination functions distinguish artificial quakes more successfully than natural ones; also, LDF provides

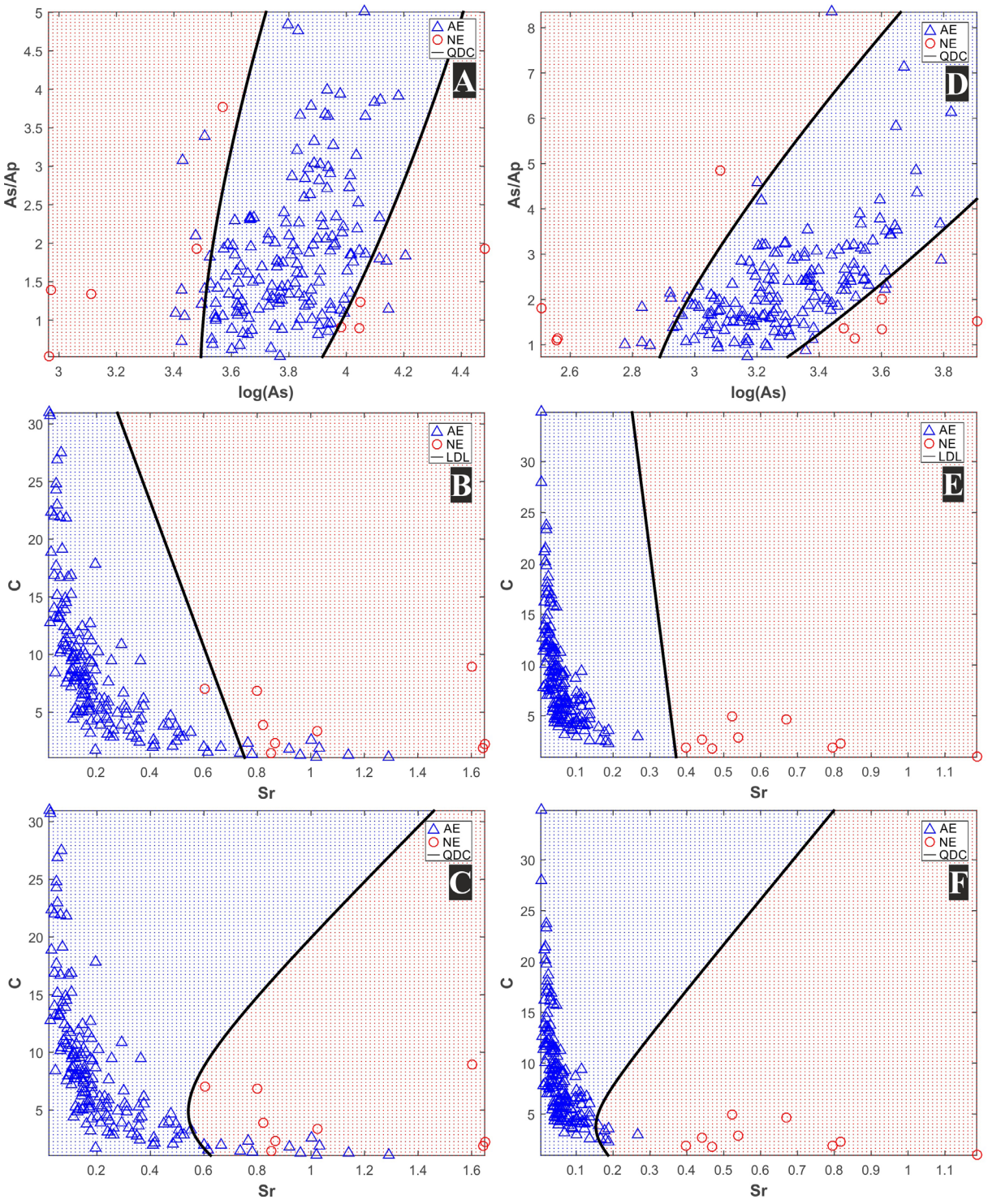

Figure 4. The results of (A) amplitude ratio method and QDF (B) complexity method and LDF (C) complexity method and QDF for station SEYD and (D) amplitude ratio method and QDF (E) complexity method and LDF and (F) complexity method and QDF for station SEDI. AE: artificial event, NE: natural event, LDL: Linear Discriminant Line, QDC: Quadratic Discriminant Curve.

more successful results than QDF according to the comparison with the FD. The success rates of the amplitude ratio method are equal to 91.53% for the statistical approach of QDF for both stations. In the complexity method, the station SEDI provides more successful results than the station SEYD with 100% and 96.05% in LDF and QDF approaches, respectively (Figure 4, Table 2). The obtained functions of the LDF and QDF for both stations are given in Table 3.

Station	Method	Statistical Approach	Number of events				Success rate (%)			Weight
			N	A	MC-N	MC-A	N	A	Overall	
–	First Det.	–	9	168	–	–	–	–	–	–
SEYD	Amp. Ratio	QDF	9	153	0	15	100.00	91.07	91.53	162.0
	Complexity	LDF	8	159	1	9	88.89	94.64	94.35	83.5
		QDF	9	155	0	13	100.00	92.26	92.66	82.0
	STFT	-	6	148	3	20	66.67	88.10	87.01	154.0
	CF-PS	-	8	145	1	23	88.89	86.31	86.44	153.0
SEDI	Amp. Ratio	QDF	9	153	0	15	100.00	91.07	91.53	162.0
	Complexity	LDF	9	168	0	0	100.00	100.00	100.00	88.5
		QDF	9	161	0	7	100.00	95.83	96.05	85.0
	STFT	-	8	167	1	1	88.89	99.40	98.87	175.0
	CF-PS	-	8	155	1	13	88.89	92.26	92.09	163.0

Table 1. The weighting values, the discrimination results of all methods and statistical approaches and their comparison with first determination for all stations. LDF: Linear Discriminant Function, QDF: Quadratic Discriminant Function, STFT: Short Time Fourier Transform, CF-PS: corner frequency-power spectrum, N: natural event, A: artificial event, MC-N misclassified natural event, MC-A misclassified artificial event.

SEYD	Amp. Ratio	$F_{QDF} = (-225.2516) + [123.2264 \quad -9.2915] * \begin{bmatrix} logA_s \\ A_s/A_p \end{bmatrix} + [logA_s \quad A_s/A_p] * \begin{bmatrix} -16.8178 & 1.3445 \\ 1.3445 & -0.1591 \end{bmatrix} * \begin{bmatrix} logA_s \\ A_s/A_p \end{bmatrix}$
	Complexity	$F_{LDF} = 14.5013 + [-18.8355 \quad -0.2993] * \begin{bmatrix} Sr \\ C \end{bmatrix}$
	Complexity	$F_{QDF} = (1.3389) + [6.0308 \quad -0.1530] * \begin{bmatrix} Sr \\ C \end{bmatrix} + [Sr \quad C] * \begin{bmatrix} -11.8147 & -0.2896 \\ -0.2896 & 0.0479 \end{bmatrix} * \begin{bmatrix} Sr \\ C \end{bmatrix}$
SEDI	Amp. Ratio	$F_{QDF} = (-136.7186) + [91.3922 \quad -11.3847] * \begin{bmatrix} logA_s \\ A_s/A_p \end{bmatrix} + [logA_s \quad A_s/A_p] * \begin{bmatrix} -15.2416 & 1.9838 \\ 1.9838 & -0.2845 \end{bmatrix} * \begin{bmatrix} logA_s \\ A_s/A_p \end{bmatrix}$
	Complexity	$F_{LDF} = 53.1432 + [-141.9930 \quad -0.5002] * \begin{bmatrix} Sr \\ C \end{bmatrix}$
	Complexity	$F_{QDF} = (2.6659) + [76.4767 \quad -1.7650] * \begin{bmatrix} Sr \\ C \end{bmatrix} + [Sr \quad C] * \begin{bmatrix} -430.8984 & -1.5778 \\ -1.5778 & 0.2968 \end{bmatrix} * \begin{bmatrix} Sr \\ C \end{bmatrix}$

Table 2. The discrimination method-based functions of station SEYD and SEDI.

Then STFT was performed on all waveforms for both SEDI and SEYD. About STFT, the dominant frequency is decisive in the source type analysis. While different dominant frequencies are observed depending on continuous-time for natural events, this situation is more stable especially in near-source artificial quakes. In spectrograms, the *S* wave phase is dominant in tectonic events, and the *P* wave phase and/or high amplitude Rayleigh waves (*Rg*) are dominant in artificial quakes. Thus, source type determination analyzes can be applied with the spectrograms [Yılmaz et al., 2013; Budakoğlu and Horasan 2018; Yavuz et al., 2019b; Tian et al., 2022]. The study analyzed the source types by focusing on the spectrograms of all waveforms recorded at both stations. When the results are compared with the FD, the success rates are calculated as 87.01% and 98.87% for stations SEYD and SEDI, respectively (Table 2, Appendix A). Four different examples of the waveforms and spectrograms of the natural and artificial quakes are given in Figure 5.

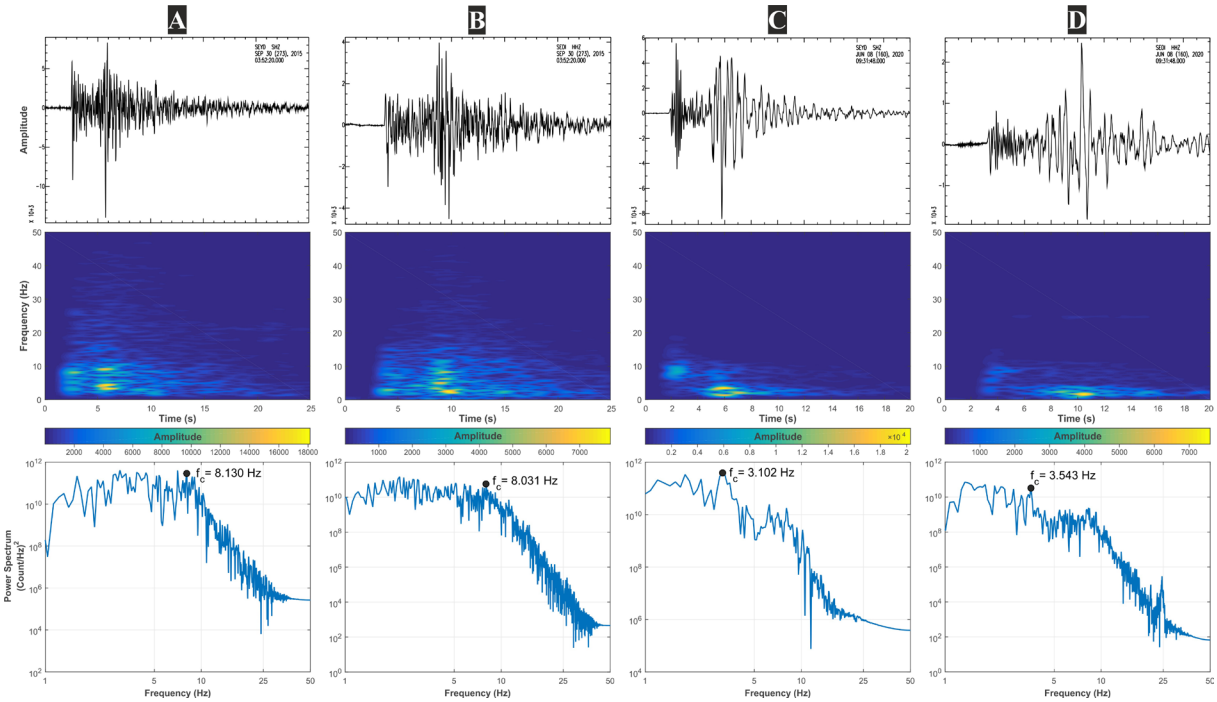

Figure 5. The waveforms, spectrograms, power spectra and corner frequencies of Sep 30, 2015 03:52:17 (UTC) natural quake at station (A) SEYD and (B) SEDI and June 08, 2020 09:31:46 (UTC) artificial quake at station (C) SEYD and (D) SEDI.

Finally, the corner frequencies and the power spectrum plots for all waveforms were calculated. The energy density of artificial events decreases more sharply towards increasing frequencies, while it is more stable on tectonic events [Su et al., 1991; Shashidhar et al., 2014; Yavuz et al., 2019a]. Thus, the corner frequencies where the energy density starts to decrease, could also have different values in various seismic event types. Lower values from the determined corner frequencies correspond to artificial and higher values to natural quakes (Figure 5). Energy variations of the different types of seismic events could easily be determined by the corner frequency values and the overall power spectra. For power spectra, the source types of artificial and natural quakes can be identified with the level of energy decrease after the corner frequency value (Figure 6). The general success rate of the power spectrum due to the corner frequencies for the station SEYD station was calculated as 86.44% and for the station SEDI station as 92.09% (Table 2, Appendix A). Four different examples of the waveforms' power spectra and their corner frequencies of the natural and artificial quakes are given in Figure 5.

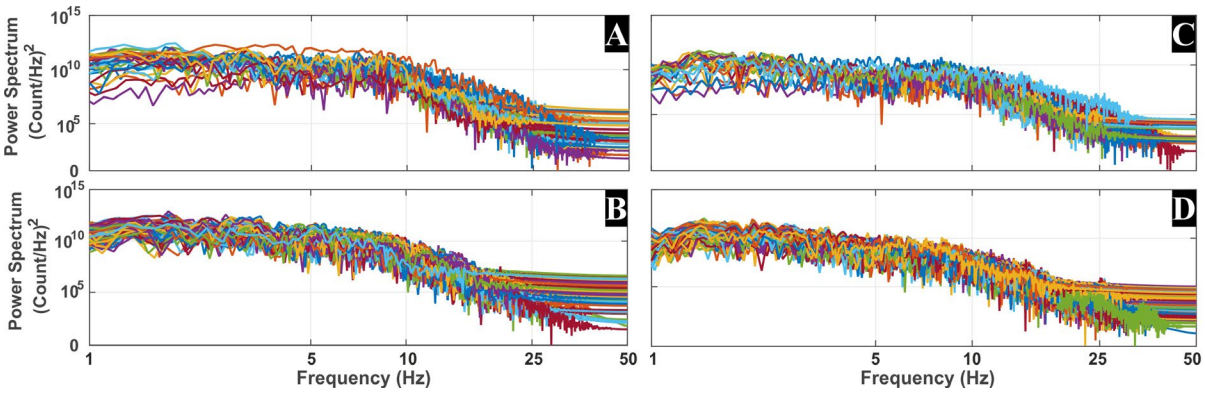

Figure 6. The power spectrum of the (A) natural and (B) artificial quakes for station SEYD and (C) natural and (D) artificial quakes for station SEDI.

The most successful result of 100% was obtained within the LDF analysis based on the complexity method performed for the station SEDI. The most unsuccessful result was obtained in the corner frequency/power spectrum analysis applied for the station SEYD as 86.44%. As a result of comparing all methods with FD, the general success rate was calculated as over 90% (Table 2). Considering success rates, the weighting values were determined for each method and statistical approach on a station basis. The number of correct data provided as a result of comparing each technique or statistical analysis with FD determines the weight of the belonging method. The weighting values for the LDF and QDF used for the complexity method were calculated by dividing them into two since the method was used in two different statistical approaches (Table 2). Each seismic event has a record of two different stations. As a result of each method and statistical approaches applied for each waveform, the weighting values are calculated based on the obtained source type. This value is calculated over the amount obtained from comparing the results of each method with the FD by subtracting the number of erroneous data from the total number of events. Since LDF and QDF are used together in the complexity method, only the weighting value of these two approaches is calculated by halving (Table 2). The source types of the events were interpreted by finding the percentage equivalents of these values (Appendix A). The source type weighting results for 177 events are shown in Figure 7.

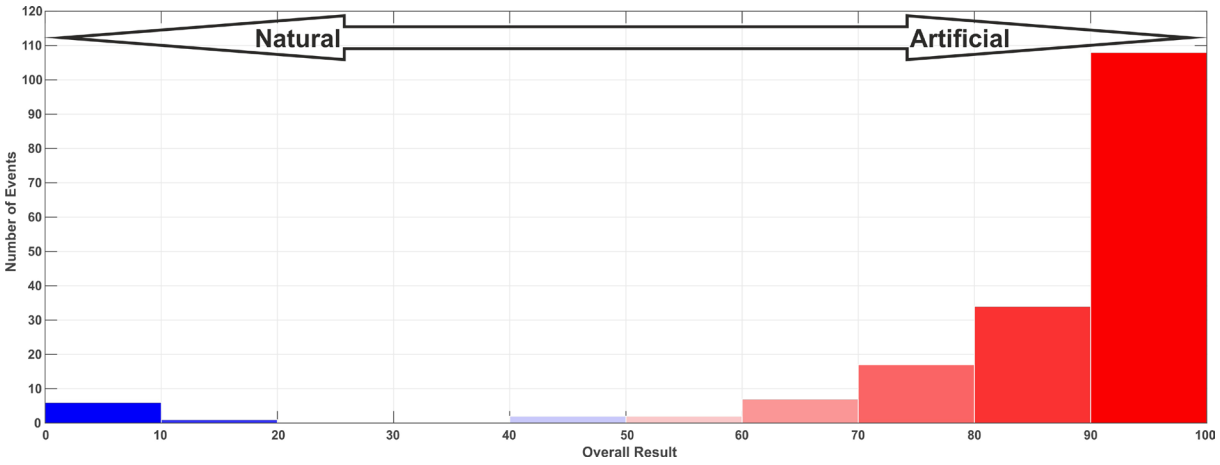

Figure 7. Number of events versus overall weight information of all events.

The same results were plotted on the map according to the AFAD, KOERI-RETMC and FD epicenters (Figure 8).

5. Conclusion and discussion

In this study, four methods and two statistical approaches used in two of these methods were performed to the data of the station SEYD and SEDI operated by KOERI-RETMC and AFAD, respectively. Since the source types of common events are defined differently in the KOERI-RETMC and AFAD catalogs, analyzes were made by determining a single source type with FD at the beginning. Source type determination analysis was performed for 177 seismic events scanned in the catalogs of both seismological centers with the help of method and station-based weighting values. The natural or artificial weight of each seismic event was determined, and the identification was defined of the source types by percent. This is the first study to determine the percentage of source types of seismic events by weighting values. Specifying source types in percentages is more reliable, especially in cataloging low-magnitude events.

According to the success rates of the methods, the most successful method is the QDF approach of the complexity method applied to the signals at the station SEDI as 100%. The lowest success rate is calculated as 86.44% in the CF-PS method applied to the recordings to the station SEYD. While the success rates in the methods using statistical approaches vary between 91.53% and 100%; in frequency domain methods, these values vary between 86.44% and 98.87%. Due to the statistical approaches, LDF gives more successful results than QDF for each station. In addition, for the frequency domain methods, the STFT technique provides more successful results than the CF-PS method

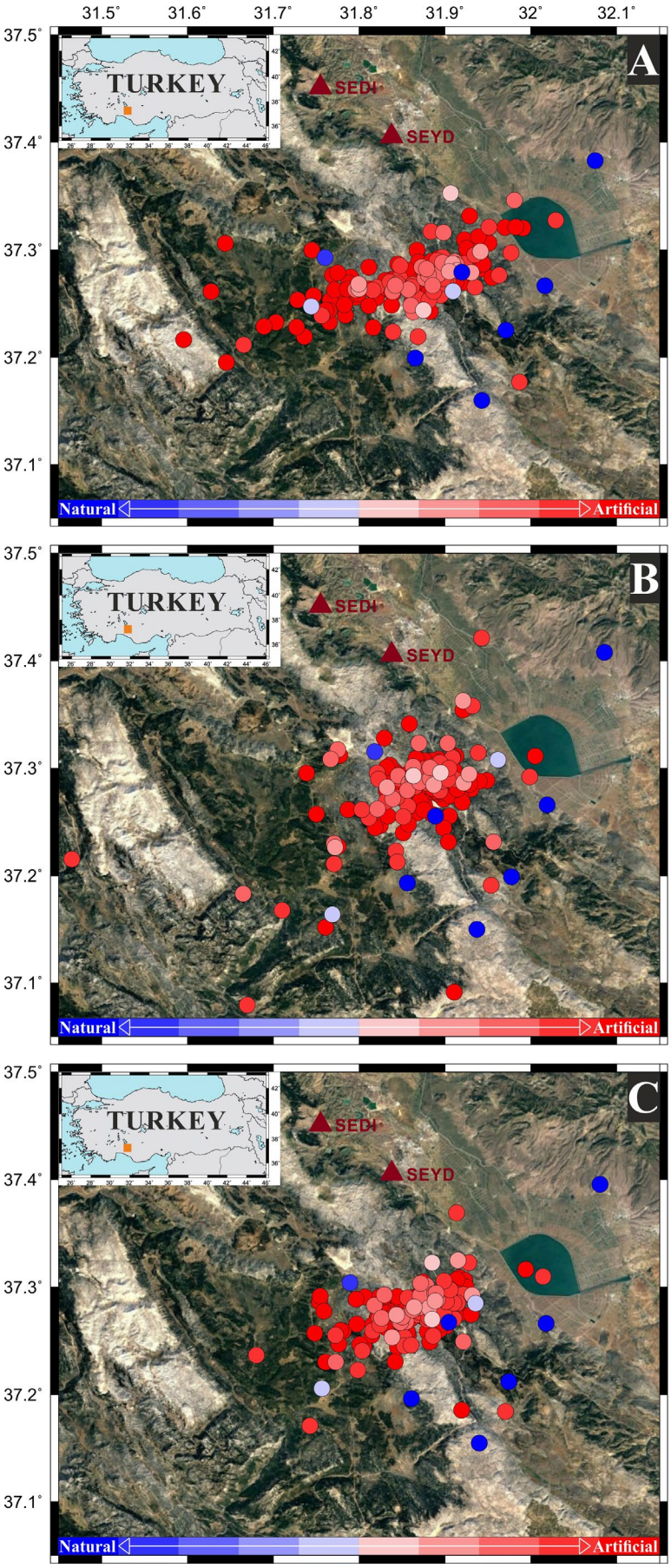

Figure 8. The epicentral final source type weighting distribution of A) KOERI-RETMC, B) AFAD and C) FD. The color flow from blue to red represents the source type of seismic events, from natural to artificial.

for each station. Therefore, performing more techniques together could increase the reliability of the identifying the source types.

To eliminate the source type differences in the KOERI-RETMC and AFAD catalogs, as in this study, many methods are used for low-magnitude seismic events, and the results are more reliable. Hence, the micro-earthquake catalogs should be refined on a common point. The accuracy and resulting reliability of the earthquake catalogs would certainly improve the understanding of Earth inner processes, especially in terms of micro-seismic activity, highlighting the crucial importance of the distinction between natural and artificial quakes.

The source type identification results of 177 events used in this study should be handled by KOERI-RETMC and AFAD. In addition, these seismological centers should identify the source types of low-magnitude events in a detailed and multi-methodical way to avoid confusion when characterizing different source types for the same seismic event. In that way, the official catalogs that form the basis of the studies such as micro-seismic activity, seismicity, seismic risk analysis, etc. will be more reliable.

Acknowledgement. The seismic waveform data can be requested from Bogazici University Kandilli Observatory and Earthquake Research Institute Regional Earthquake-Tsunami Monitoring Center (KOERI-RETMC) and Republic of Turkey Prime Ministry Disaster and Emergency Management Authority (AFAD). The figures have been prepared by using the GMT software (Wessel and Smith, 1998), MATLAB2015a and SAC (Goldstein et al., 2003). I would like to thank Dr. Andrea Bizzarri (sector editor) and anonymous reviewers for their crucial and helpful comments.

References

Akbaş, B., N. Akdeniz, A. Aksay, İ. E. Altun, V. Balcı, E. Bilginer, T. Bilgiç, M. Duru, T. Ercan, İ. Gedik, Y. Günay, İ. H. Güven, H. Y. Hakyemez, N. Konak, İ. Papak, Ş. Pehlivan, M. Sevin, M. Şenel, N. Tarhan, N. Turhan, A. Türkecan, Ü. Ulu, M. F. Uğuz and A. Yurtsever (2011). 1:1.250.000 ölçekli Türkiye Jeoloji Haritası, Maden Tetkik ve Arama Genel Müdürlüğü Yayını, Ankara-Türkiye (in Turkish).

Aki, K. (1995). Discriminating underground explosions from earthquakes using seismic coda waves, University of Southern California Los Angeles Center for Earth Sciences.

Allmann, B. P., P. M. Shearer and E. Hauksson (2008). Spectral discrimination between quarry blasts and earthquakes in Southern California, Bull. Seism. Soc. Am., 98, 4, 2073-2079.

Arai, N. and Y. Yosida (2004). Discrimination by short-period seismograms, International Institute of Seismology and Earthquake Engineering, Building Research Institute (IISEE), Lecture Note, Global Course, Tsukuba, Japan, 10.

Arrowsmith, S. J., M. D. Arrowsmith, M. A. Hedlin and B. Stump (2006). Discrimination of delay-fired mine blasts in Wyoming using an automatic time-frequency discriminant, Bull. Seism. Soc. Am., 96, 6, 2368-2382.

Ataeva, G., Y. Gitterman and A. Shapira (2017). The ratio between corner frequencies of source spectra of P-and S-waves—a new discriminant between earthquakes and quarry blasts, J. Seismol., 21, 1, 209-220.

Auger, F., P. Flandrin, P. Goncalves and O. Lemoine (1996). Time-Frequency Toolbox for Use with Matlab: reference Guide, CNRS, France.

Badawy, A., M. Gamal, W. Farid and M. S. Soliman (2019). Decontamination of earthquake catalog from quarry blast events in northern Egypt, J. Seismol., 23, 6, 1357-1372.

Beck, S. L. and T. C. Wallace (1997). Broadband seismic recordings of mining explosions and earthquakes in South America, University of Arizona, Department of Geosciences, Arizona, USA.

Başokur, A. T. (2007). Spektral analiz ve sayısal süzgeçler, TMMOB Jeofizik Mühendisleri Odası Eğitim Yayınları (in Turkish).

Baumgardt, D. R. and G. B. Young (1990). Regional seismic waveform discriminants and case-based event identification using regional arrays, Bull. Seism. Soc. Am., 80, 1874–1892.

Bormann, P. (2009). New Manual of Seismological Observatory Practice (NMSOP-1), IASPEI, GFZ German Research Centre for Geosciences, Potsdam.

Brune, J. N. (1970). Tectonic stress and the spectra of seismic shear waves from earthquakes, J. Geophys. Res., 75, 26, 4997-5009.

Budakoğlu, E. and G. Horasan (2018). Classification of seismic events using linear discriminant function (LDF) in the Sakarya region, Turkey, Acta Geophysica, 66, 5, 895-906.

Carr, D. B and H. D. Garbin (1998). Discriminating ripple-fired explosions with high-frequency (>16 Hz) data, Bull. Seism. Soc. Am., 88, 4, 963-972.

Cohen, L. (1989). Time-frequency distributions: a review, Proceedings of the Institute of Electrical and Electronics Engineers (IEEE) 77:941–981.

Emre, Ö., T. Y. Duman, S. Özalp, H. Elmacı, Ş. Olgun and F. Şaroğlu (2013). Açıklamalı Türkiye Diri Fay Haritası. Ölçek 1:1.250.000, Maden Tetkik ve Arama Genel Müdürlüğü, Özel Yayın Serisi-30, Ankara-Türkiye. ISBN: 978-605-5310-56-1 (in Turkish).

Fisher, R. A. (1936). The use of multiple measurements in taxonomic problems, Ann. of Eugen, 7, 2, 179-188.

Frank, V. and V. Hlavac (2004). Statistical pattern recognition toolbox for Matlab, User Guide, Prague, Czech: Center for Machine Perception, Czech Technical University.

Gaber, H., S. Elkholy, M. Abdelazim, I. H. Hamama and A. S. Othman (2017). Seismological investigation of September 09 2016, North Korea underground nuclear test, NRIAG Journal of Astronomy and Geophysics, 6, 2, 278-286.

Gabor, D. (1946). Theory of communication, Journal of the Institution of Electrical Engineers (IEE) 3:429–457.

Gitterman, Y. and T. Eck (1993). Spectra of quarry blasts and microearthquakes recorded at local distances in Israel, Bull. Seism. Soc. Am., 83, 6, 1799-1812.

Gitterman, Y., V. Pinsky and A. Shapira (1998). Spectral classification methods in monitoring small local events by the Israel seismic network, J. Seismol., 2, 3, 237-256.

Gitterman, Y. and A. Shapira (1993). Spectral discrimination of underwater explosions, Isr. J. Earth Sci., 42, 1, 37-44.

Goldstein, P., D. Dodge, M. Firpo and L. Minner (2003). SAC2000: Signal processing and analysis tools for seismologists and engineers. In: Lee WHK, Kanamori H, Jennings PC, Kisslinger C (eds) Invited contribution to "The IASPEI international handbook of earthquake and engineering seismology, Academic Press, London.

Hedlin, M. A, J. B. Minster and J. A. Orcutt (1989). The time-frequency characteristics of quarry blasts and calibration explosions recorded in Kazakhstan, USSR, Geophys. J. Int., 99, 1, 109-121.

Hedlin, M. A, J. B. Minster and J. A. Orcutt (1990). An automatic means to discriminate between earthquakes and quarry blasts, Bull. Seism. Soc. Am., 80, 6B, 2143-2160.

Horasan, G., A. B. Güney, A. Küsmezer, F. Bekler, Z. Öğütçü and N. Musaoğlu (2009). Contamination of seismicity catalogs by quarry blasts: An example from Istanbul and its vicinity, northwestern Turkey, J. Asian Earth Sci., 34, 1, 90-99.

Kelly, E. J. (1968). A study of two short-period discriminants, Massachusetts Inst. of Tech., Lexington Lincoln Lab.

Kartal, Ö. F. and G. Horasan (2011). Trabzon ve civarındaki deprem ve patlatma verilerinin birbirinden ayırt edilmesi, SAÜ Fen Bilimleri Dergisi, 15, 1, 68-74 (in Turkish).

Kekovalı, K., D. Kalafat and P. Deniz (2012). Spectral discrimination between mining blasts and natural earthquakes: Application to the vicinity of Tunçbilek mining area, Western Turkey, Int. J. Phys. Sci., 7, 35, 5339-5352.

Kim, W. Y., D. W. Simpson and P G. Richards (1994). High-frequency spectra of regional phases from earthquakes and chemical explosions, Bull. Seism. Soc. Am., 84, 5, 1365-1386.

Koch, K. and D. Fäh (2002). Identification of Earthquakes and Explosions Using Amplitude Ratios: The Vogtland Area Revisited, Pure Appl. Geophys., 159, 4, 735–757.

Korrat, I. M., A. Lethy, M N. ElGabry, H M. Hussein and A. S. Othman (2022). Discrimination Between Small Earthquakes and Quarry Blasts in Egypt Using Spectral Source Characteristics, Pure Appl. Geophys., 179, 2, 599-618.

Krzanowski, W. J. (1988). Principles of multivariate analysis: a user's perspective, Clarendon.

Kuyuk, H. S., E. Yildirim, E. Dogan and G. Horasan (2014). Clustering seismic activities using linear and nonlinear discriminant analysis, J. Earth Sci., 25, 1, 140-145.

Öğütçü, Z., G. Horasan and D. Kalafat (2011). Investigation of microseismic activity sources in Konya and its vicinity, central Turkey, Nat. Hazards, 58,1, 497-509.

Pyle, M. L. and W. R. Walter (2019). Investigating the Effectiveness of P/S Amplitude Ratios for Local Distance Event Discrimination, Bull. Seism. Soc. Am., 109, 3, 1071-1081.

Roueff, A., J. Chanussot, J. I. Mars and M. Q. Nguyen (2004). Unsupervised separation of seismic waves using the watershed algorithm on time scale images, Geophys. Prospect., 52, 4, 287-300.

Seber, G. A. F. (1984). Multivariate Observations, Hoboken, John Wiley & Sons, 1984.

Semmlow, J. (2012). The Fourier transform and power spectrum, In Signals, and Systems for Bioengineers, Academic, 253-268.

Sertçelik, F. and O. Başer (2010). Güney Ege Bölgesi'nde yapay ve doğal kaynaklı titreşimlerin ayırt edilmesi, Yerbilimleri, 31, 3, 141-168 (in Turkish).

Sertçelik, F., E. Yavuz, M. Birdem and G. Merter (2020). Discrimination of the natural and artificial quakes in the Eastern Marmara Region, Turkey, Acta Geod. Geophys., 55, 4, 645-665.

Shashidhar, D., K. Mallika, N. P. Rao, H. V. S. Satyanarayana and H. K. Gupta (2014). Detection of quarry blasts in the Koyna-Warna region, western India, Open J. Earthquake Res., 3, 04, 162.

Stein, S. and M. Wysession (2009). An introduction to seismology, earthquakes, and earth structure, John Wiley & Sons.

Su, F., K. Aki and N. N. Biswas (1991). Discriminating quarry blasts from earthquakes using coda waves, Bull. Seism. Soc. Am., 81, 1, 162-178.

Tan, A., G. Horasan, D. Kalafat and A. Gülbağ (2021). Discrimination of earthquakes and quarries in the Edirne district (Turkey) and its vicinity by using a linear discriminate function method and artificial neural networks, Acta Geophysica, 69, 1, 17-27.

Tian, X., M. Wang, X. Zhang, X. Wang, S. Sheng and J. Lü (2022). Discrimination of earthquake and quarry blast based on multi-input convolutional neural network, Chinese Journal of Geophysics, 5, 1802-1812.

Tibi, R., K. D. Koper, K. L. Pankow and C. J. Young (2018a). Depth discrimination using Rg-to- Sg spectral amplitude ratios for seismic events in Utah recorded at local distances, Bull. Seism. Soc. Am., 108, 3A, 1355-1368.

Tibi, R., K. D. Koper, K. L. Pankow and C. J. Young (2018b). Discrimination of Anthropogenic Events and Tectonic Earthquakes in Utah Using a Quadratic Discriminant Function Approach with Local Distance Amplitude Ratios, Bull. Seism. Soc. Am., 108, 5A, 2788-2800.

Tüysüz, N. and G. Yaylalı (2005). Jeoistatistik Kavramlar ve Bilgisayarlı Uygulamalar, Karadeniz Teknik Üniversitesi Yayınları, Trabzon (in Turkish).

Wessel, P. and W. H. F. Smith (1998). New, improved version of generic mapping tools released, EOS Trans. Am. Geophys., 79, 47, 579.

Wüster, J. (1993). Discrimination of chemical explosions and earthquakes in central Europe—a case study, Bull. Seism. Soc. Am., 83, 1184–1212-

Yavuz, E., F. Sertçelik, H. Livaoğlu, H. Woith and B. G. Lühr (2019a). Discrimination of quarry blasts from tectonic events in the Armutlu Peninsula, Turkey, J. Seismol., 23, 1, 59-76.

Yavuz, E., F. Sertçelik, H. Livaoğlu and T. S. Irmak (2019b). Gaziantep-Kahramanmaraş Bölgesinde meydana gelen deprem ve taş ocağı patlatmalarının zaman ve frekans ortamı yöntemleri ile sınıflandırılması (Classification of quarry blasts and tectonic events with time and frequency domain methods in Gaziantep-Kahramanmaras Region, Turkey), Bitlis Eren Üniversitesi Fen Bilimleri Dergisi, 8, 2, 642-651 (in Turkish).

Yavuz, E. (2021). AFAD zayıf yer hareketi istasyonları bazlı doğal ve yapay kaynaklı sarsıntı ayrımının yapılması ve kaynak türünü belirleyen yazılım algoritmasının tasarlanması (Discrimination of natural and artificial quakes based on AFAD weak ground motion stations and designing a software algorithm for determining the source type), PhD. dissertation, Kocaeli University, Kocaeli, Turkey (in Turkish).

Yılmaz, Ş., Y. Bayrak and H. Çınar (2013). Discrimination of earthquakes and quarry blasts in the eastern Black Sea region of Turkey, J. Seismol., 17, 2, 721-734.

***CORRESPONDING AUTHOR: Evrim YAVUZ**,
Istanbul Metropolitan Municipality, Department of Earthquake Risk Management and Urban Improvement,
Directorate of Earthquake and Geotechnical Investigation, Bakırköy, Istanbul, Turkey,
e-mail: evrim.yavuz@ibb.gov.tr